Journal of Experimental Botany, Vol. 58, No. 8, pp. 2113–2131, 2007
doi:10.1093/jxb/erm050 Advance Access publication 8 May, 2007
This paper is available online free of all access charges (see http://jxb.oxfordjournals.org/open_access.html for further details)

Journal of Experimental Botany
www.jxb.oxfordjournals.org

RESEARCH PAPER

Stomatal regulation by microclimate and tree water relations: interpreting ecophysiological field data with a hydraulic plant model

Roman Zweifel[1,4,*], Kathy Steppe[2] and Frank J. Sterck[3]

[1] *Swiss Federal Institute for Forest, Snow and Landscape Research (WSL), Forest Ecosystem Processes, Zürcherstrasse 111, CH-8903 Birmensdorf, Switzerland*

[2] *Ghent University, Department of Applied Ecology and Environmental Biology, Laboratory of Plant Ecology, Belgium*

[3] *Wageningen University, Forest Ecology and Forest Management, The Netherlands*

[4] *University of Bern, Institute of Plant Sciences, Switzerland*

Received 22 December 2006; Revision received 15 February 2007; Accepted 22 February 2007

Abstract

Dynamics in microclimate and physiological plant traits were studied for Pubescent oak and Scots pine in a dry inner-alpine valley in Switzerland, at a 10 min resolution for three consecutive years (2001–2003). As expected, stomata tended to close with increasing drought in air and soil. However, stomatal aperture in oak was smaller than in pine under relatively wet conditions, but larger under dry conditions. To explore underlying mechanisms, a model was applied that (i) quantifies water relations within trees from physical principles (mechanistic part) and (ii) assumes that signals from light, stomatal aperture, crown water potential, and tree water deficit in storage pools control stomata (systemic part). The stomata of pine showed a more sensitive response to increasing drought because both factors, the slowly changing tree water deficit and the rapidly changing crown water potential, closed the stomata. By contrast, the stomata of oak became less drought-sensitive as the closing signal of crown water potential was opposed by the opening signal of tree water deficit. Moreover, parameter optimization suggests that oak withdrew more water from the storage pools and reduced leaf water potentials to lower levels, without risking serious damage by cavitation. The new model thus suggests how the hydraulic water flow and storage system determines the responses in stomatal aperture and transpiration to drought at time scales ranging from hours to multiple years, and why pine and oak might differ in such responses. These differences explain why oaks are more efficient competitors during drought periods, although this was not the case in the extremely dry year 2003, which provoked massive leaf loss and, from July onwards, physiological activity almost ceased.

Key words: Drought stress, *Pinus sylvestris*, *Quercus pubescens*, stomatal regulation, tree water deficit, water storage.

Introduction

Plants are located within a water potential gradient along which water and soluble compounds are passively transported. This beneficial situation for the plant can turn into a negative one when the gradient becomes too steep and causes damage either by dehydration of living cells (Larcher, 2003) or by cavitation due to tensions in the water columns of the xylem being too high (Tyree and Sperry, 1989; Brodribb and Holbrook, 2003; Sperry, 2003; Vilagrosa *et al*., 2003). Trees need, therefore, mechanisms to maintain this gradient within a non-damaging range (Bond and Kavanagh, 1999; Buckley, 2005). The most important mechanism is the regulation of the stomatal aperture, which decouples the canopy from the water-demanding atmosphere by increasing the resistance for water vapour leaving the crown (Meinzer *et al*., 1997).

* To whom correspondence should be addressed. E-mail: roman.zweifel@natkon.ch

Stomatal regulation is a complex process as it depends on how microclimate, leaf CO_2 concentration, plant hormones, leaf water potential and soil water potential (Tardieu and Davies, 1993; Whitehead, 1998; Dewar, 2002; Tuzet *et al*., 2003; Messinger *et al*., 2006) induce a variety of physiological responses that may regulate stomatal conductance (Tenhunen *et al*., 1987; Tardieu and Davies, 1993; Dodd, 2003; Thompson and Holbrook, 2004). Although isolated signalling pathways leading to stomatal opening or closure have been described in detail, the integration of this knowledge into a whole-plant-level model is far from conclusive (Buckley, 2005). The reason might be that models put a strong emphasis on leaf-level processes. Leaf-level models for trees may be satisfactory when soil moisture is adequate, but usually they fail in simulating patterns of transpiration and conductance when the soil water potential is very low or when it is fluctuating over a wide range (Leuning, 1995; Dewar, 2002; Hanson *et al*., 2004).

Besides other factors, leaf water potential has been recognized as playing a key role in stomatal regulation (Comstock and Mencuccini, 1998; Bond and Kavanagh, 1999; Brodribb and Holbrook, 2003). The gradient between leaf and root water potential is kept below a threshold, as to avoid the negative effects of cavitation on water flow and, ultimately, on carbon gain (Tyree, 1988; Sperry *et al*., 2002; Brodribb and Holbrook, 2003; Buckley, 2005). The cohesion–tension theory (Dixon and Joly, 1894) and the resistance flow model (van den Honert, 1948) describe a tree as an integrated hydraulic system and predict water potential gradients, water fluxes, and leaf water potentials within plants. More recent physiological tree models integrated water storage pools into an extended, hydraulic system (Perämäki *et al*., 2001; Zweifel *et al*., 2001; Messinger *et al*., 2006; Steppe *et al*., 2006), and thus provided better predictions for diurnal patterns of water flow, water potentials, and water storage in plants. Beyond its influence on flow dynamics and water potentials, water storage as a measure of plant water deficit (Hinckley and Lassoie, 1981; Zweifel *et al*., 2005) may affect the regulation of stomatal aperture via plant hormones in a similar way to the signalling from dry soil to the stomata as suggested by Dodd (2003). Zweifel *et al*. (2002) combined microclimatic factors with feedback signals from tree water relations to explain the midday depression of *Picea abies*. Tuzet *et al*. (2003) may be the first to develop a physiological whole-plant-model that integrated most factors to predict stomatal regulation in drought-stressed plants. Their approach, however, has a few drawbacks: the mathematical structures are not easy to interpret in terms of physiological factors contributing to stomatal regulation (Buckley *et al*., 2003), water storage was not included in their hydraulic system, and the predictions were not tested against field data.

In this study, a unique set of data is explored with detailed measurements of air/soil microclimate and tree physiology over three years at a 10 min resolution, covering a wide range of drought conditions including the exceptionally hot and dry summer 2003. This data set allowed stomatal aperture values of an evergreen conifer (*Pinus sylvestris* L.) and a deciduous ring-porous tree species (*Quercus pubescens* Willd.) to be estimated. First, the distinctly varying stomatal responses of the two species to different severities of drought on diurnal, weekly, and seasonal timescales, and between years, are shown. Second, the performance was tested of a tree model that simulates these species-specific ecophysiological field measurements from a mechanistic integrated hydraulic system (including water storage and water potential gradients) and empirically weighted feedback signals from light, stomatal aperture, leaf water potentials, and tree water deficit. The model used (i) to evaluate how the hydraulic system and the joint effects of different signals contribute to dynamics in transpiration, storage, water potential gradients, and, ultimately, stomatal aperture on various times scales, and (ii) to produce hypotheses about the different patterns of water use and stomatal dynamics between the two tree species.

Materials and methods

Ecophysiological field study

Study sites and trees: The study site was located in an open oak–pine woodland near Salgesch on the south-facing slope of the main valley of the Wallis, Switzerland (46°19′27" N, 7°34′40" E, 975 m asl). Central Wallis is an inner-alpine valley characterized by a dry climate. This is mainly caused by inner-valley shielding. The valley is oriented SE–NW with regard to the main storm tracks from the West and wet air masses from the South. Mean annual precipitation over the past 20 years was about 600 mm per year. Annual precipitation at the site of measurement was 752 mm in 2001, 899 mm in 2002, and 495 mm in 2003.

Pubescent oak (*Quercus pubescens* Willd.) and Scots pine (*Pinus sylvestris* L.) were the most abundant tree species and juniper (*Juniperus communis* L.) was the most abundant woody shrub in the vegetation of this very dry site. Whereas some oaks were up to 110-years-old, 95% of them were younger than 70 years. Most of the dominant pines were between 100-years-old and 150-years-old (Zweifel *et al*., 2005). The investigated woody species stood in one of the typical patches of trees (32 m^2 in area), consisting of oaks, pines, *Viburnum lantana,* and *J. communis*, surrounded by grass and bare rock. The eight selected trees represented mature individuals of the study site with estimated ages between 50 years and 120 years. The height of the six selected oaks and the two selected pines ranged between 3.5–4.0 m and 3.5–5.0 m, respectively, the stem diameter between 7.2–9.5 cm and 11.9–23.2 cm, respectively, and the crown projection area on the ground between 8 m^2 and 18 m^2 for both species. The soil on this steep south-facing slope (~25°) was shallow with a maximum depth of 0.1–0.3 m at the site of measurement. Below the organic material was a mostly solid rock layer.

Climate data: Climate data were collected at the site with a solar-powered logging and steering-system (IPS, University of Bern, Switzerland and Markasub AG, Switzerland). The heart of the

system was a logger (CR10X, Campell, UK). Details about sensor types and installation are described in Zweifel *et al.* (2006). Microclimate was resolved into north-exposed and south-exposed canopy and in conditions outside of the vegetation. Microclimate data were used as input to run the model (Appendix A).

The data set covered the relatively wet years of 2001 and 2002 and the hot and dry year of 2003 (Table 1). The years 2001 and 2002 were rather similar in terms of their averaged climatic conditions, but in 2002 there was a remarkable drought period in the last three weeks of June which led to very low Ψ_{Soil}, conditions not comparable with those in 2001. The weather conditions in 2003 led to large water deficits in the soil and plants even before the leaves of oak flushed at the end of April. From mid-July onwards, the activity of the trees of both species ceased completely and came back to a low percentage only in September. The leaves of oak had already turned yellow and brown in July and some trees flushed a few leaves in September.

Sap flow measurements: Sap flow was continuously assessed at small north-exposed and south-exposed branches on five oaks and two pines by heat balance gauges (Dynagage, Dynamax, USA). A detailed description about the distribution of sap flow gauges within the forest patch can be found in Zweifel *et al.* (2006).

Estimation of stomatal aperture from field measurements: Stomatal aperture of the leaves of small branches was estimated from continuous measurements of branch sap flow (which is assumed to represent branch transpiration) and microclimate by computing the ratio between actual (F_{Branch}) and potential transpiration (F_{Pot_Branch}). Since this ratio is mainly (but not only) changed by the stomatal conductance (Hsiao and Acevedo, 1974; Wright *et al.*, 2003), $F_{Branch}/F_{Pot\_Branch}$ can be used as a good approximation for the degree of stomatal aperture (as a percentage) (Zweifel *et al.*, 2002, 2006). The measured values of $F_{Branch}/F_{Pot\_Branch}$ were averaged and scaled up to the entire crown (θ_E). This estimated θ_E was compared with modelled stomatal aperture (θ) which was independently achieved by applying the model described below.

A crucial point in this procedure is to calculate the potential transpiration of branches from microclimate. Potential evaporation for a homogenous vegetation surface can be estimated by the single-leaf model (Penman, 1948; Monteith, 1965). To use this concept for three-dimensional objects, for example, individual branches of trees (F_{Pot_Branch}), the single leaf model was modified by Zweifel *et al.* (2002). In their model, microclimate (solar radiation, wind speed, vapour pressure deficit, and air temperature) and the geometric properties of the branch determine the potential transpiration. F_{Pot_Branch} is calculated as:

$$F_{Pot\_Branch} = \frac{\Delta s \times ((Rad \times \chi)W_H) + \rho \times c_p \times \frac{(VPD)}{r_a}}{\Delta s + \gamma \times (1 + \frac{r_{s\,min}}{r_a})} \times \frac{k}{\lambda} \times Z_T \quad (1)$$

Table 1. *Mean daytime values (6 h–20 h) of microclimatic factors at Salgesch, Switzerland*

Temperature (T), solar radiation (Rad), vapour pressure deficit (VPD), soil water potential (Ψ_{Soil}) (seasonal minimum in brackets) and sum of rain (24 h) over the vegetation period (15 May to 30 September) of the years 2001 to 2003.

	T [°C]	Rad [W m^{-2}]	Rain [mm]	Ψ_{Soil} [kPa]	VPD [kPa]
2001	19.1	409	472	–76 (–167)	0.89
2002	19.5	394	696	–82 (–283)	0.89
2003	23.1	417	401	–186 (–448)	1.45

where Δs is the slope of the saturation vapour pressure curve at the actual temperature (T), Rad is net radiation flux, W_H is heat flux between the tree and the soil, ρ is air density, c_p is specific heat of the air, γ is the psychrometer coefficient, $r_{s\,min}$ is canopy resistance with fully opened stomata, r_a is aerodynamic boundary layer resistance to heat and water vapour diffusion and depends on the boundary layer thickness (δ) of the crown surface, Z_T is the idealized crown (branch) surface, χ is the ratio of sunlit to shaded parts of Z_T (χ=0.01: crown completely shaded; χ=0.5: crown completely in the sun), k is the conversion factor to the unit g h^{-1} per crown (k=60×60×1000), and λ is the latent heat of vaporization of water. The parameters Z_T, χ, and $r_{s\,min}$ were found according to the procedure described in Zweifel *et al.* (2002).

Leaf water potential: Water potentials of needles and leaves (Ψ_{leaf}) were measured with a pressure chamber (SKPM 1400, SKYE Instruments, UK). Two to five samples were measured per record and the average of these measurements was used for further analyses. Day courses (about ten records per day) of Ψ_{leaf} were available for six days in 2002 and 2003.

Stem radius changes and tree water deficit: Stem radius changes (ΔR) were measured with point dendrometers (ZB01, Markasub AG, Switzerland) on six oaks and two pines (Zweifel *et al.*, 2006). The dendrometers were mounted at 0.5 m above ground on the hillside (north) of each stem. The electronic part of the dendrometer was mounted on a carbon fibre frame which was fixed to the stem by three stainless steel threaded rods implanted into the heartwood. The sensing rod was slightly pressed against the tree stem by a spring. The contact point of the dendrometer head was positioned 1–6 mm into the bark surface, but still within the outermost dead layer of the bark. The sensitivity of the dendrometers to temperature and humidity was negligible due to the use of a weather-insensitive carbon frame and a temperature-insensitive electronic transformer (Weggeberpotentiometer LP-10F, Pewatron, Switzerland). The electronical resolution of the dendrometers in combination with the logger used was 0.4 μm.

Stem radius changes have two main components, radial growth and water-related swelling and shrinkage of the stem with water content (Daudet *et al.*, 2005; Zweifel *et al.*, 2005). Zweifel *et al.* (2005) suggested an algorithm to separate the course of ΔR into these main components. ΔR de-trended for growth represents the tree water deficit (ΔW) as introduced by Hinckley and Lassoie (1981). Absolute ΔW values typically range from 0 μm (fully hydrated state) to about 800 μm, proportional to the reduction in stem diameter due to dehydration of storage pools. ΔW represents the water status of the entire tree since all water-carrying living parts of a tree are hydraulically interlinked and pressure changes are therefore transmitted and levelled (with a certain delay).

Scaled measurements: Microclimatic conditions, physiological measurements (e.g. branch sap flow) and physiological estimations from measurements (e.g. potential branch transpiration or estimated stomatal aperture) were either collected in the south-exposed or the north-exposed crown part of eight tree individuals. These measurements were averaged for these two expositions and scaled to an 'average tree' of Pubescent oak and Scots pine. These virtual trees consisted of 70% south-exposed branches and 30% north-exposed branches, the leaf area was 25 m^2 and 30 m^2 for oak and pine, respectively. This corresponded to a site-typical tree individual with about 4 m in height and a cross-sectional area at the stem base of about 230 cm^2 for both species (Zweifel *et al.*, 2005). These scaled data were used to parameterize the model and to compare with the model output. Appendix A lists all the parameters and declares their property in terms of data acquisition and utilization in the model.

Model structure

The general modelling concept: A dynamic ecophysiological tree model was developed and applied to explore how the integrated hydraulic system, including water storage in stem and crown, influences stomatal aperture and transpiration of the two species (Fig. 1). The model needs potential transpiration of the crown (F_{Pot}), light intensity (*Rad*), and soil water potential (Ψ_{Soil}) to be run. In addition to these data, a set of dynamic physiological measurements (transpiration or sap flow, leaf water potential, and stem radius changes) over at least two weeks is needed to parameterize the model.

The model tree consists of root, stem, crown, and water storage compartments. Based on physical principles, water fluxes between root and stem, between stem xylem and other tree components, and between crown and air are formalized (Fig. 1a; Appendix A). Further, the model calculates how the dynamics in stomatal aperture are explained from empirically weighted signals by light (*Rad*), stomatal aperture (θ), crown water potential (Ψ_{Crown}), and tree water deficit (ΔW). These signals allow an interpretation of how much a certain measure in tree water relations contributes to stomatal regulation but they do not *a priori* refer to one of the specific pathways mentioned in the literature (Davies and Zhang, 1991; Dodd, 2003; Eisinger *et al*., 2003; Buckley, 2005).

Flow and storage system: The water flow and storage processes are based on hydraulic and electrical circuit principles. An overview about the flow and storage model components is given in Fig. 1 and a short description including the applied mathematical formulations are given in Appendix B. Detailed descriptions can be found in Zweifel *et al*. (2001) and Steppe *et al*. (2006).

Transpiration: The current transpiration (F_{Transp}) is the potential transpiration (F_{Pot}) down-regulated by the stomatal aperture θ. This is formulated as:

$$F_{Transp} = \theta \times F_{Pot} \quad (2)$$

Stomatal regulation: Model stomata directly respond to signals from light intensity (*Rad*), crown water potential (Ψ_{Crown}), tree water deficit (ΔW) and the current stomatal aperture (θ) (Fig. 1). These signals have opposing effects on θ. The sum of all the empirically weighted signals together determines whether the stomatal aperture remains the same (signal=0), increases (signal >0), or decreases (signal <0).

Ψ_{Crown} always introduces a closing signal on the stomata proportional to its actual value, whereas *Rad* and ΔW can have an opening or a closing effect. In addition to these factors, the model

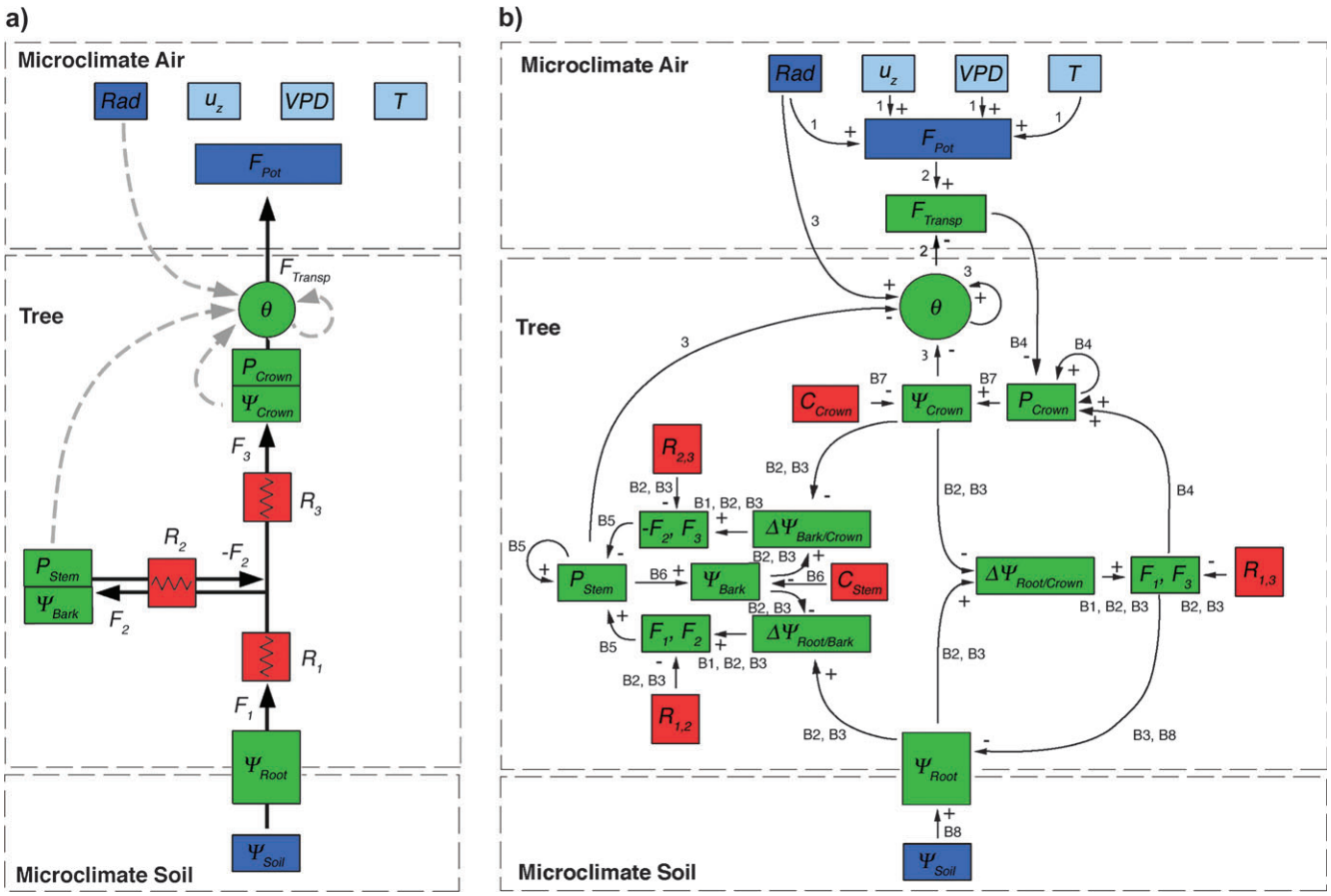

Fig. 1. (a) The model is based on hydraulic flow and storage principles with the components: water storage in stem (mainly the bark) (P_{Stem}) and crown (P_{Crown}), flow path with corresponding water fluxes (F_1 to F_3), flow resistances (R_1 to R_3), and the corresponding water potentials (Ψ). Variables are calculated (green), parameters are optimized (red), and input factors were measured (blue). Light-blue elements are input factors for the calculation of the potential transpiration (F_{Pot}), and dark-blue elements are input parameters for the tree water relations model. (b) The interrelations of the model components are indicated by labelled arrows. Labels refer to the equations 1–3 and B1–B8. Arrows carrying the symbol '+' indicate a positive correlation between the related elements, '–' a negative one. Abbreviations are listed in Appendix A.

introduces a dependency on the current θ. Thus, stomatal aperture is formulated as:

$$\theta_{t=i} = \theta_{t=i-1} + \Psi_{Crown} \times \Phi_{Crown} + \Delta W \times \Phi_{Bark} + \frac{Rad - \Gamma_{Rad}}{\Gamma_{Rad}} \Phi_{Rad} \quad (3)$$

where $\theta_{t=i}$ is the stomatal aperture at the time i, $\theta_{t=i-1}$ is the stomatal aperture at the previous iteration step, Φ_{Crown}, Φ_{Bark}, and Φ_{Rad} are weighting factors of the signals induced by Ψ_{Crown}, ΔW, and Rad on θ, and Γ_{Rad} is a light threshold.

The model was forced to have the following two constraints for equation 3:

$$0 = < \theta = < 1 \quad (3a)$$

and

$$\frac{Rad - \Gamma_{Rad}}{\Gamma_{Rad}} \Phi_{Rad} \leqslant \Phi_{Rad} \quad (3b)$$

where equation 3a makes sure that θ remains within the possible range of stomatal aperture between 0 and 1 (i.e. 0% and 100%), and equation 3b formulates the ideas that (i) $Rad < \Gamma_{Rad}$ proportionally increases the closing-signal, that (ii) Rad between Γ_{Rad} and $2\Gamma_{Rad}$ proportionally increases the opening-signal, and that (iii) $Rad > 2\Gamma_{Rad}$ induces a constant opening-signal ($=\Phi_{Rad}$) on θ.

The model equations 2 and 3 are in many ways interlinked with the flow and storage equations B1 to B8 (Appendix B). As a consequence, the model design builds a network of feedback loops between components of tree water relations and the stomatal aperture. The entire network with all the mechanistic and empirical interrelations based on these equations is depicted in Fig. 1b. Dynamic variables in the system (green) are calculated from other variables, optimized parameters (red) and microclimatic input factors (blue). Due to this recursive, systemic nature of the model, every component involved has at least an indirect effect on stomatal regulation. The model was run on a time step of 10 min for three subsequent growth seasons (2001–2003).

Model parameterization and tests

Sensitivity analysis: The sensitivity analysis of the model covered two aspects: (i) the model sensitivity on variations of the parameters to select the parameters driving most of the variability in model output and (ii) the degree of independency of individual parameters to test whether pairs of parameters were compensating each other. A detailed description of the sensitivity analysis including the corresponding results is given in Appendix C.

Parameterization: The model contains nine parameters to be optimized (Appendix A), four parameters which are pre-set from estimations or measurements (Appendix C) and three variables as model inputs (Rad, F_{Pot}, and Ψ_{Soil}). All the tree-internal variables as flow rates (F_{Transp}, F_1, F_2, and F_3), water potentials (Ψ_{Root}, Ψ_{Bark}, and Ψ_{Crown}), water contents (P_{Stem} and P_{Crown}), and stomatal aperture (θ) are the result of the model calculations. Four variables, measured by independent methods, were used to optimize the model output to fit the 10-min interval measurements: manually measured Ψ_{Leaf} versus modelled Ψ_{Crown}, scaled continuous measurements of branch sap flow F_{Branch} versus modelled F_{Transp}, ΔW (deduced from measured ΔR values) versus modelled changes of ΔP_{Stem}, and estimated versus modelled θ (equation 3).

Nine parameters to be optimized in a single procedure seem to be a high number, but the parameters can be unambiguously determined (see sensitivity analysis in Appendix C) when having a temporally highly resolved (⩽1 h) data set containing dynamic information about leaf water potential, sap flow, and tree water deficit (stem radius changes) for at least 2 weeks (plus the microclimatic conditions needed to run the model). Such a set of data is strongly limiting the range in which every parameter can vary. If one of the parameters is set outside of this range, the dynamics of the virtual tree collapse and the model is thus not able to simulate the measurements any more (results not shown). In particular, maximum and minimum leaf water potential data are important for finding definite parameter values because they define, together with measured soil water potential, the maximum steepness of water potential gradients and, consequently, all the properties of water movement directly affecting water uptake, water storage dynamics, and, indirectly, stomatal control. In general, the information content of 3–4 independently measured variables as a time series is, in almost all cases, high enough to identify nine parameters of a recursive model.

In this investigation, every year's set of data for oak and pine was divided into two periods: May to July and August to September. This arrangement led to two sets of parameters per species and year (Table 2) and allowed a test to made of how consistent the parameters were within the same season and over three years. Further, the optimized parameters could be compared between the two species and provided biological information on species-specific drought responses, for example, flow resistances, or amount of consumed water from internal storages, etc.

Best-fit estimates for the parameters were found by an iterative procedure (Solver, Excel) which optimized the average value of the modelling efficiency factors (EF_m, see Appendix C) for the four sets of measured data (Ψ_{Crown}, F_{Transp}, ΔW, and θ). The modelling efficiency statistic was calculated according to Mayer and Butler (1993) and Hanson *et al.* (2004):

$$EF_m = 1 - \frac{\sum |y_i - \bar{y}_i|}{\sum |y_i - \bar{y}|} \quad (4)$$

where $\bar{y}_i$ is the model value at the time i, y_i is the measured value at the time i, and $\bar{y}$ is the measured average value of the factor m.

Statistical evaluations: To evaluate the 'goodness-of-fit' of the model simulations for Ψ_{Crown}, F_{Transp}, ΔW, and θ, different statistical measures were used according to tests proposed by Hanson *et al.* (2004). In addition to EF_m, mean bias (*Bias*) and mean absolute bias (*ABS*) were calculated from the following equations (Reynolds, 1984; Walters, 1994):

$$Bias = \frac{\sum (y_i - \bar{y}_i)}{n} \quad (5)$$

$$ABS = \frac{\sum |y_i - \bar{y}_i|}{n} \quad (6)$$

Bias provides a direct measure of the tendency for over- or under-prediction (positive or negative values, respectively). The *ABS* value is a measure of the mean deviation from the observed values. The *EF* value is similar to the calculated r^2-value in conventional linear regression, but it uses the one-to-one relationship rather than the regression line as the reference (Hanson *et al.*, 2004). An *EF* value of 1 represents a perfect fit and values range from 1 to infinitely negative. *EF* values of 1, however, are not expected because of natural variability and experimental error associated with data collection. In this paper, *EF* values are based on data sets with 10 min resolution which lowers *EF* in comparison to data sets with hourly or daily resolution. As a point of reference, *EF* values >0.25 were considered as in satisfactory agreement with measured data.

Table 2. *List of model parameters optimized for sets of half-season data*

Statistically significant differences of the mean parameter values between the two species are indicated by an asterisk (*t* test, $P < 0.05$). SD, standard deviation. Abbreviations and units are listed in Appendix A.

	May–Jul 01	Aug–Sep 01	May–Jul 02	Aug–Sep 02	May–Jul 03	Aug–Sep 03	Mean[a]	SD[a]
Quercus pubescens								
$R_{1,3}$	0.0006	0.0005	0.0005	0.0005	0.0010	0.0139	0.0006	0.0002*
R_2	0.11	0.14	0.12	0.11	0.11	0.21	0.12	0.01
Γ_{Rad}	92.4	87.3	62.3	61.6	16.5	15.8	64.0	26.9*
Φ_{Bark}	0.349	0.370	0.327	0.306	0.122	0.186	0.295	0.089*
Φ_{Rad}	0.204	0.205	0.192	0.195	0.292	0.269	0.218	0.038*
k_1	4.74	3.34	4.32	4.83	7.54	8.77	4.96	1.40
k_2	0.92	0.79	1.16	1.19	0.95	1.10	1.00	0.15
C_{Crown}	93.4	98.1	93.9	86.3	98.2	61.8	94.0	4.3*
C_{Stem}	122.6	110.6	143.0	141.9	86.2	78.8	120.9	21.2
Pinus sylvestris								
$R_{1,3}$	0.0002	0.0002	0.0004	0.0005	0.0004	0.0011	0.0003	0.0001*
R_2	0.12	0.06	0.09	0.11	0.02	0.03	0.08	0.04
Γ_{Rad}	32.5	37.9	26.3	22.2	4.9	5.3	24.8	11.3*
Φ_{Bark}	–0.032	–0.033	–0.035	–0.034	–0.032	–0.037	–0.033	0.001*
Φ_{Rad}	0.102	0.104	0.143	0.135	0.144	0.077	0.126	0.019*
k_1	6.39	4.78	16.85	14.21	2.19	2.56	8.88	5.65
k_2	1.27	1.17	1.90	1.77	0.50	0.56	1.32	0.50
C_{Crown}	204.1	222.2	146.6	117.8	135.0	124.6	165.1	40.7*
C_{Stem}	269.1	245.9	137.4	146.6	136.7	172.3	187.1	58.0

[a] Mean and SD without data of the second half of 2003.

Results

Measured physiological responses

The stomatal response to microclimate strongly varied with increasing drought and showed significant differences between the two species investigated (Fig. 2). In general, drought closed the stomata. However, this response to drought was not linear. Under moderately wet conditions trees opened their stomata at twilight in the morning and only little down-regulation was detected during the day. With ceasing daylight the stomata usually closed, but Scots pine in particular sometimes showed night-time transpiration. Under dry conditions both species showed the typical pattern of midday depression when stomata opened in the morning, were closing before noon, and reopened in the evening. Under extreme drought conditions, the stomata only partially opened in the morning and very soon completely closed for the rest of the day. When comparing days 4 and 5 in Fig. 2, the effect of increased tree water deficit on stomatal aperture becomes distinctly visible: the microclimatic conditions of these two days were very similar, whereas tree water deficit was significantly higher on day 5 inducing a more distinct stomatal closure for both species. Besides this non-linearity against an increase in drought stress, there were distinctly differing stomatal response patterns of the two species observed: Scots pine had relatively more opened stomata in wet conditions whereas Pubescent oak had relatively more opened stomata in dry conditions. Further, there was a less severe drought stress level needed to induce a complete closure of the stomata in Scots pine than in Pubescent oak.

On a weekly scale, this species-specific stomatal response became particularly obvious for drought periods with a following rehydration by a heavy rain (Fig. 3). The course of stomatal aperture of oak remained significantly above zero for all daylight hours, whereas that of pine went towards zero and remained very low from before noon and for the rest of the day. After the rain on 28 June, the stomata of both species opened much more the next day and the two patterns became similar again.

On an annual scale, a comparison of mean daily stomatal aperture values between Pubescent oak and Scots pine clearly showed that the broadleaved species was able to keep its stomata open significantly longer than the co-occurring coniferous species during drought (Fig. 4). The degree of mean daily stomatal aperture of Pubescent oak was kept above 25% until a tree water deficit of about 450 μm, whereas Scots pine fell below this percentage at about 200 μm. The course of tree water deficit was quite similar for both species over the three years investigated (Fig. 5). Even in the extreme summer of 2003 when the oak leaves wilted at the end of July, the corresponding tree water deficit did not become significantly different for the two species in the following weeks.

Differences in the physiological response between Pubescent oak and Scots pine appeared not only in stomatal aperture but also in crown water potential and sap flow. The range of crown water potentials of oak was

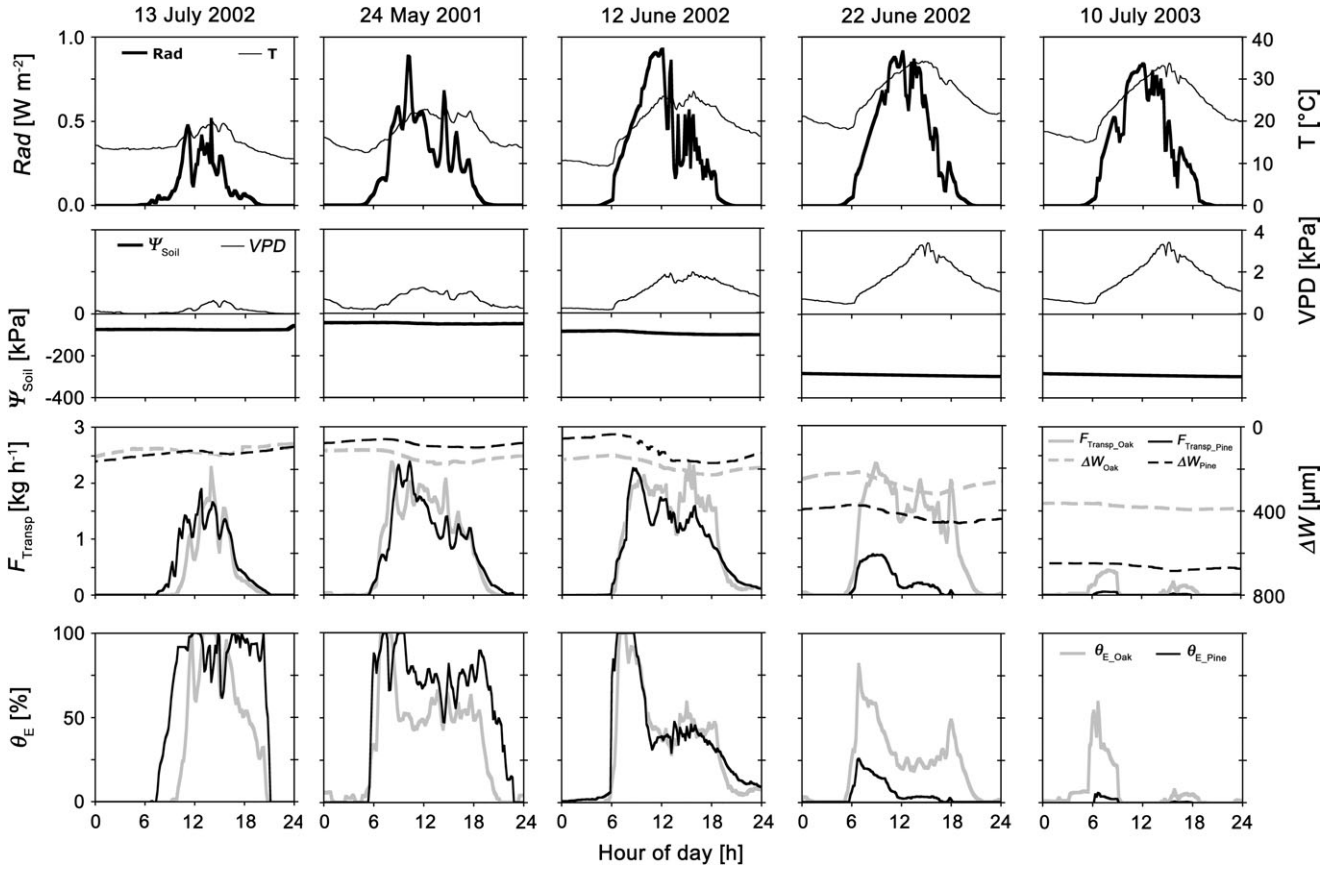

Fig. 2. Measurements on five days with different drought stress: 13 July 2002 was a cloudy day in a relatively wet period, 24 May 2001 was a partially sunny day in a relatively wet period, 12 June 2002 was sunny in the morning and cloudy in the afternoon in a moderately dry period, 22 June 2002 was a sunny day in a very dry period, and 10 July 2003 was a sunny day in an extremely dry period. Diurnal courses of stomatal aperture (θ_E) of Pubescent oak (grey lines) and Scots pine (black lines) strongly vary with the severeness of drought. *Rad*, radiation; *T*, air temperature; Ψ_{Soil}, mean daytime values (6–20 h) for soil water potential; *VPD*, vapour pressure deficit of the air; F_{Transp}, transpiration; and ΔW, tree water deficit.

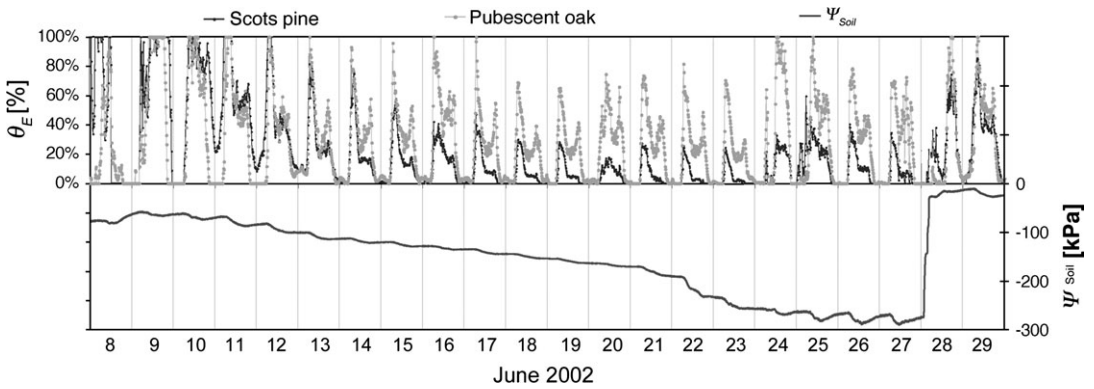

Fig. 3. Measurements in a drought period over 20 days in June 2002: the stomata of both species open less with the ongoing drought, however, the stomatal aperture (θ_E) of Scots pine is much more affected than θ_E of Pubescent oak. With the rain on 28 June soil water potential (Ψ_{Soil}) releases and θ_E increases again.

about the double (0 to –4.8 MPa) as the one of pine (0 to –2.7 MPa) (Table 3). Corresponding to the faster stomatal closure of pine after reaching a daily maximum in the late morning (e.g. Fig. 2, 12 June 2002), the diurnal course of pine sap flow usually showed a more distinct flow peak than that of oak.

Model performance

The tree model successfully simulated 10-min stomatal aperture values and flow and storage dynamics of the two tree species over three years. The model caught short-term responses over days as well as long-term dynamics of the drought and heat periods over months (Fig. 6). And the

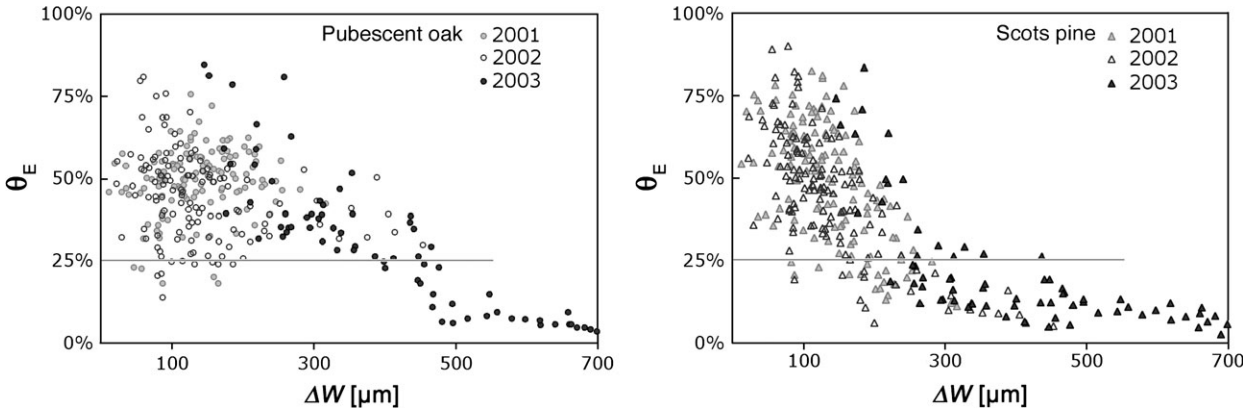

Fig. 4. Mean daily stomatal aperture values (θ_E) of Pubescent oak and Scots pine related to the corresponding tree water deficits (ΔW) over three years.

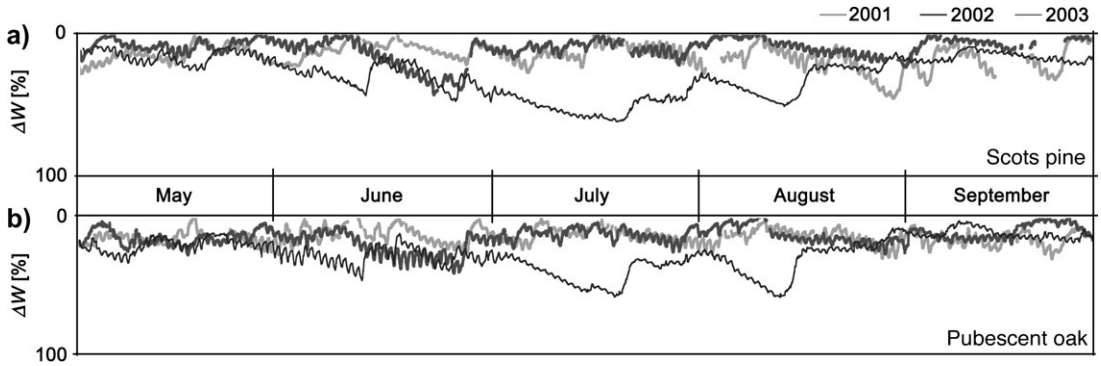

Fig. 5. Courses of relative tree water deficits (ΔW) of (a) Scots pine and (b) Pubescent oak over the three seasons 2001 to 2003.

Table 3. *Characteristic physiological measures of oak* (Quercus pubescens) *and pine* (Pinus sylvestris)

Transpiration (F_{Transp}), maximum sap flow in the lower stem section ($F_{1\ max}$), maximum water exchange rate between stem and bark ($F_{2\ max}$), maximum depletion of the crown ($\Delta P_{Crown\ max}$) and the bark ($\Delta P_{Bark\ max}=\Delta W_{max}$), minimum crown water potential ($\Psi_{Crown\ min}$), minimum tree water potential ($\Psi_{Bark\ min}$), minimum root water potential ($\Psi_{Root\ min}$), and stomatal aperture (θ).

	2001 Measured	2001 Modelled	2002 Measured	2002 Modelled	2003 Measured	2003 Modelled	
F_{Transp} *Quercus* (sum of season)	2051	1960	1969	2164	476	469	[kg]
F_{Transp} *Pinus* (sum of season)	1871	1848	1527	1614	330	254	[kg]
$F_{1\ max}$ *Quercus*	n.m.[a]	3251	n.m.	3938	n.m.	2133	[g h^{-1}]
$F_{1\ max}$ *Pinus*	n.m.	3516	n.m.	3637	n.m.	2335	[g h^{-1}]
$F_{2\ max}$ *Quercus*	n.m.	8.4	n.m.	9.5	n.m.	10.2	[g h^{-1}]
$F_{2\ max}$ *Pinus*	n.m.	8.4	n.m.	13.7	n.m.	10.4	[g h^{-1}]
$\Delta P_{Crownmax}$ *Quercus*	n.m.	374	n.m.	369	n.m.	491	[g]
$\Delta P_{Crownmax}$ *Pinus*	n.m.	401	n.m.	441	n.m.	350	[g]
$\Delta P_{Barkmax}$ *Quercus*	177	140	233	224	307	247	[g]
$\Delta P_{Barkmax}$ *Pinus*	160	180	261	255	278	315	[g]
$\Psi_{Crownmin}$ *Quercus*	n.m.	−3.8	−2.9	−3.9	−3.8	−4.8	[MPa]
$\Psi_{Crownmin}$ *Pinus*	n.m.	−1.8	−1.6	−2.2	−1.7	−2.7	[MPa]
$\Psi_{Barkmin}$ *Quercus*	n.m.	−1.3	n.m.	−1.6	n.m.	−3.5	[MPa]
$\Psi_{Barkmin}$ *Pinus*	n.m.	−0.6	n.m.	−1.5	n.m.	−1.6	[MPa]
$\Psi_{Rootmin}$ *Quercus*	n.m.	−1.1	n.m.	−1.5	n.m.	−3.6	[MPa]
$\Psi_{Rootmin}$ *Pinus*	n.m.	−0.7	n.m.	−1.3	n.m.	−1.6	[MPa]
θ *Quercus* (mean)	28%	22%	27%	30%	13%	11%	[%]
θ *Pinus* (mean)	32%	25%	30%	28%	9%	6%	[%]

[a] n.m., Not measured.

most important point, the model was able to reproduce the observed species-specific patterns.

The simulations, obtained by applying the parameters in Table 2 for the corresponding periods, were analysed in terms of their quality to explain transpiration (F_{Transp}), stomatal aperture (θ), tree water deficit (ΔW), and leaf water potential (Ψ_{Leaf}). The parameterization process was forced to find a solution for an optimum overall mean

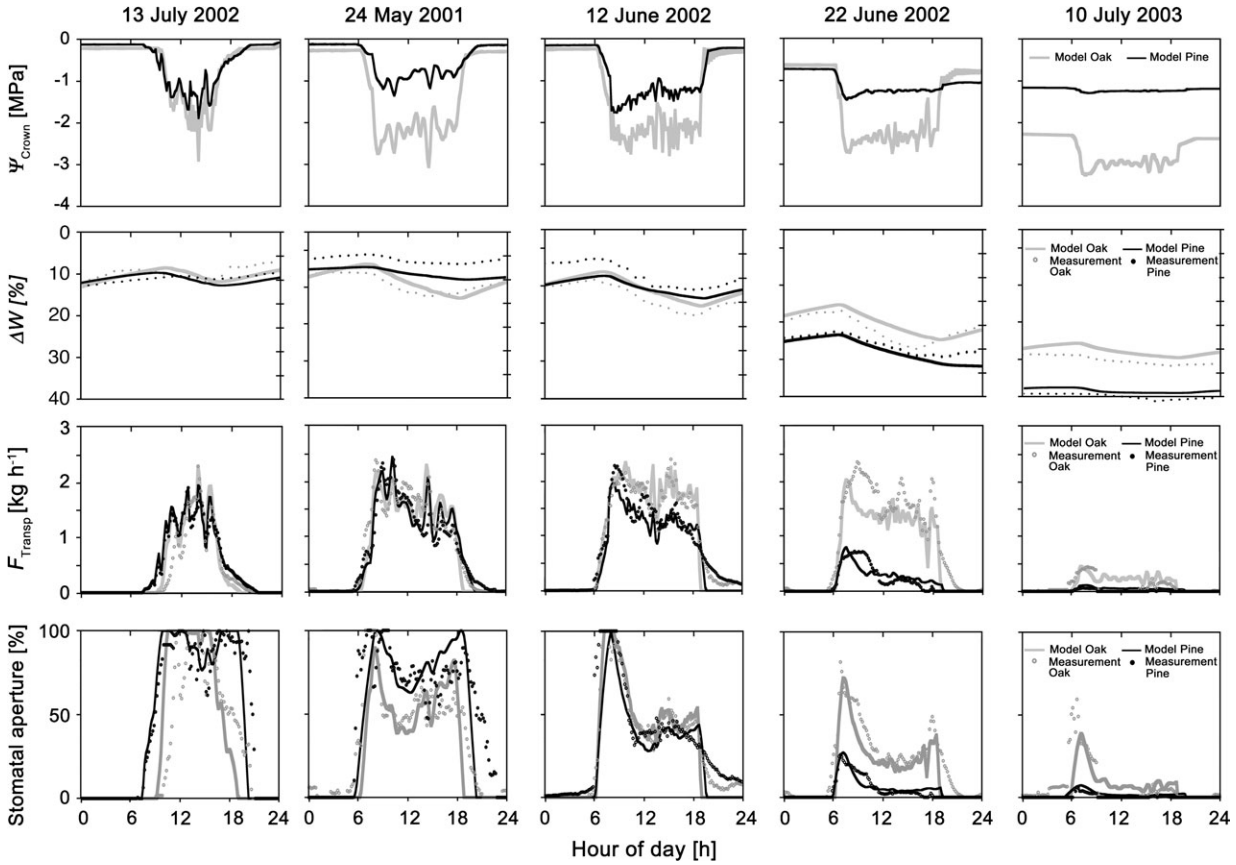

Fig. 6. Comparisons between measured and modelled courses of physiological factors for the same days as shown in Fig. 2. Black symbols represent Scots pine, grey symbols represent Pubescent oak, circles indicate measurements, and lines show model predictions: crown water potentials Ψ_{Crown}, tree water deficit ΔW, crown transpiration F_{Transp}, and stomatal aperture (θ).

Table 4. *Statistical evaluations of the 'goodness-of-fit' between simulation and measurement of transpiration* (F_{Transp}), *tree water deficit* (ΔW), *crown water potential* (Ψ_{Crown}), *and stomatal aperture* (θ)

Bias, *ABS,* and *EF* are calculated according to equations 4–6.

	2001				2002				2003			
	n	*Bias*	*ABS*	*EF*	*n*	*Bias*	*ABS*	*EF*	*n*	*Bias*	*ABS*	*EF*
Quercus pubescens												
F_{Transp} [g h^{-1}]	18459	–42.54	184.80	0.74	18752	46.08	214.43	0.69	19808	–2.30	88.08	0.54
ΔW [μm]	18558	0.00	0.02	0.32	19945	0.00	0.02	0.52	20015	0.00	0.03	0.58
Ψ_{Crown} [MPa]	0	n.m.[a]	n.m.	n.m.	26	0.04	0.34	0.54	48	–0.11	0.48	0.35
θ [%]	18372	–0.06	0.11	0.53	18752	0.02	0.13	0.53	19808	–0.02	0.08	0.52
Average				0.53				0.57				0.50
Pinus sylvestris												
F_{Transp} [g h^{-1}]	18362	–15.48	203.71	0.68	18176	0.28	186.70	0.64	20015	–22.80	78.74	0.43
ΔW [μm]	17593	0.00	0.03	0.35	18127	0.00	0.02	0.48	20015	0.02	0.05	0.46
Ψ_{Crown} [MPa]	0	n.m.[a]	n.m.	n.m.	15	–0.03	0.15	0.87	37	0.01	0.14	0.37
θ [%]	18341	–0.05	0.15	0.40	18121	–0.02	0.14	0.49	19975	–0.03	0.07	0.50
Average				0.48				0.62				0.44

[a] n.m., Not measured.

simulation quality (*EF*) for all four variables measured (Tables 3, 4). *EF* changed slightly between years and species, but an overall *EF* value >0.44 suggests that the simulations provided good predictions for all variables measured (Table 4).

The simulations were precise enough to distinguish between the species-specific θ and F_{Transp} responses of oak and pine to the same microclimatic conditions (Fig. 6). Oak characteristically regulated its transpiration rate to a level, which was kept more or less constant over the

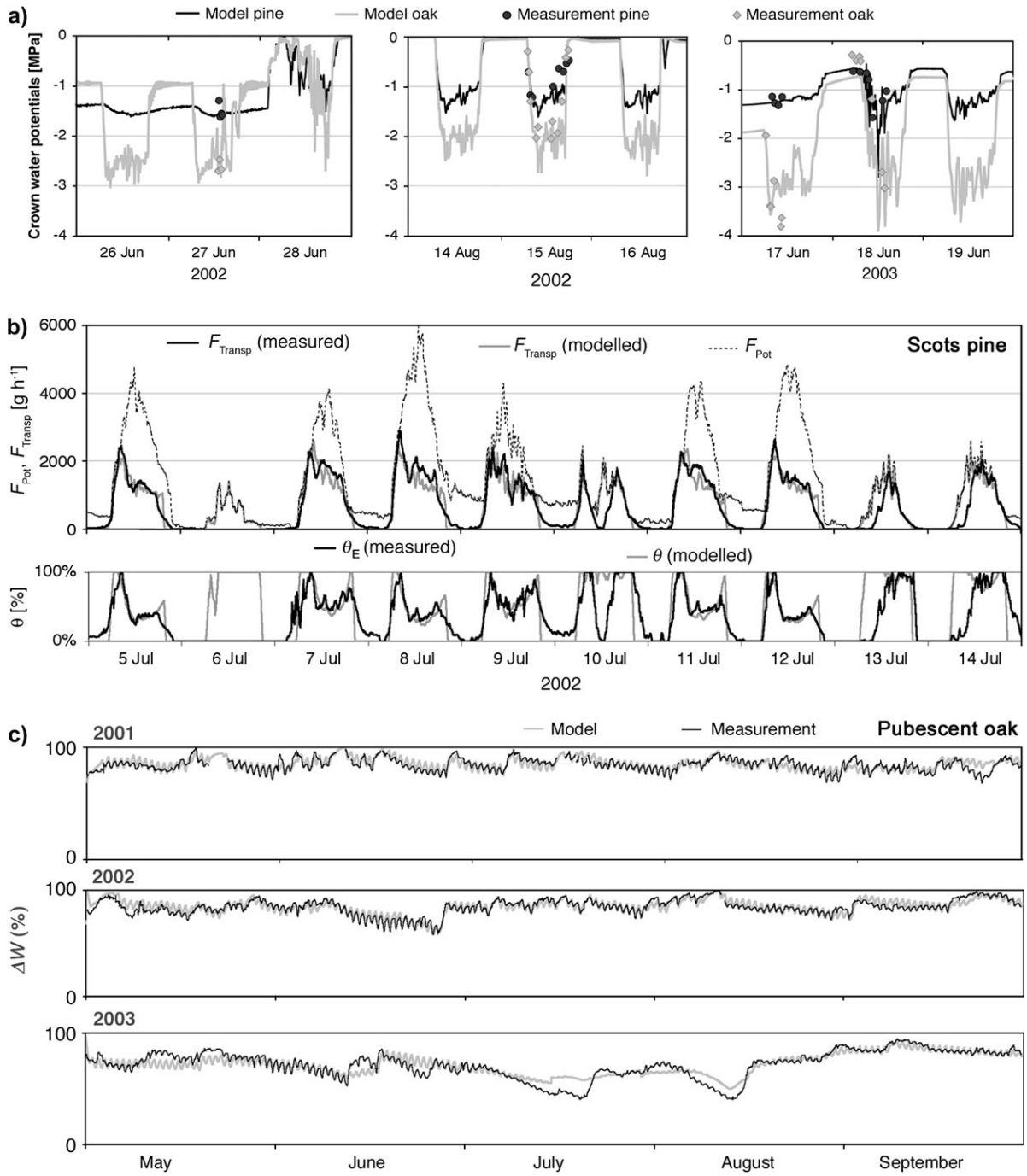

Fig. 7. A selection of comparisons between measured and modelled courses of physiological factors (a) on a diurnal scale, (b) on a weekly scale, and (c) on a seasonal scale. (a) Measured (circles and squares) and modelled (lines) courses of crown water potentials of Pubescent oak (grey symbols) and Scots pine (black symbols). (b) Measured and modelled crown transpiration F_{Transp} in combination with estimated potential transpiration F_{Pot} of Scots pine. Estimated stomatal aperture (θ_E) is compared with modelled stomatal aperture (θ). (c) Measured and modelled tree water deficits (Δ*W*) of Pubescent oak.

day, whereas pine showed a distinct sap flow peak in the morning followed by a decreasing course over the day (Figs 6, 7b). Deviations larger than the average occurred for night-time transpiration of Scots pine, which were not caught by the model (Fig. 7b).

The general courses of tree water deficit of both species were simulated very well for the three seasons (Fig. 7c). Deviations larger than average occurred in September 2001, in June 2002 (pine) and in July and August 2003. Increased deviations occurred usually, when Ψ_{Soil} was poorly correlated to ΔW or in other words when ΔW was lowered after little rain but this rain did not affect Ψ_{Soil} (or was not sensed by the equitensiometers). In general, the simulated crown water potentials fitted the small number of measured data from 2002 and 2003 very well (Fig. 7a; Table 4). However, deviations between model and measurement occurred in cases where measured leaf water potentials (oak) reached extreme negative values, which were underestimated by the model simulation (e.g. 17 June 2003, Fig. 7a). The distinct difference between the Ψ_{Crown} ranges of the two tree species was caught very well by the model (Fig. 7a; Table 3).

Model interpretations

The parameter values were found to be very consistent within a species for all half-year data sets, except for the second half of 2003 (Table 2). This exception was no surprise since the very hot and dry conditions led to early leaf senescence and a cessation of physiological activity from mid-summer onwards, which may have changed morphological and physiological properties represented in the parameters optimized: in parallel with increasing drought, there was a tendency towards an increase in R_1 ($=R_3$) and a decrease in Γ_{Rad}, C_{Crown}, and Φ_{Bark} for both species. Or in other words, the (model) trees had higher xylem flow resistances, more pronounced stomatal reactions on tree water deficit, a lower light threshold to open stomata, and less water to withdraw from the crown (per MPa^{-1}) under dry conditions than under moderate ones. Other parameters showed no consistent patterns over the years.

The mean values of the parameters were in five out of nine cases significantly different between oak and pine (Table 2). Species-specific variations of parameters were found for R_1, Γ_{Rad}, Φ_{Bark}, Φ_{Rad}, and C_{Crown}. Oak had a higher flow resistance, its stomata responded more strongly to *Rad* but needed a higher light threshold to open compared with pine. Remarkable, however, is the finding that the stomata of oak responded positively to ΔW, which means that the stomata were less (closing-) sensitive to Ψ_{Crown} at high ΔW than during well-watered conditions. Pine, in contrast, responded more sensitive to changes in Ψ_{Crown} during periods of high ΔW than during periods of saturation.

Development of (model-) water potentials during a drought

Oak and pine responded with a general decrease in predawn water potentials with increasing drought and both species gradually decreased their root water potentials to more negative values when the soil was drying (Fig. 8). Since root water potentials decreased more rapidly than soil water potentials, the water potential gradients over the soil–root depletion zone became steeper as the soil dried. In addition to the general pattern, there were also distinct species–specific differences in the courses of water potentials. Since oak was able to keep its stomata partially open all day even, for example, during the driest time of the drought period in 2002 (Figs 3, 8), it maintained a water potential gradient between roots and crown (Fig. 8), remained able to withdraw water from the soil, and continued to transpire.

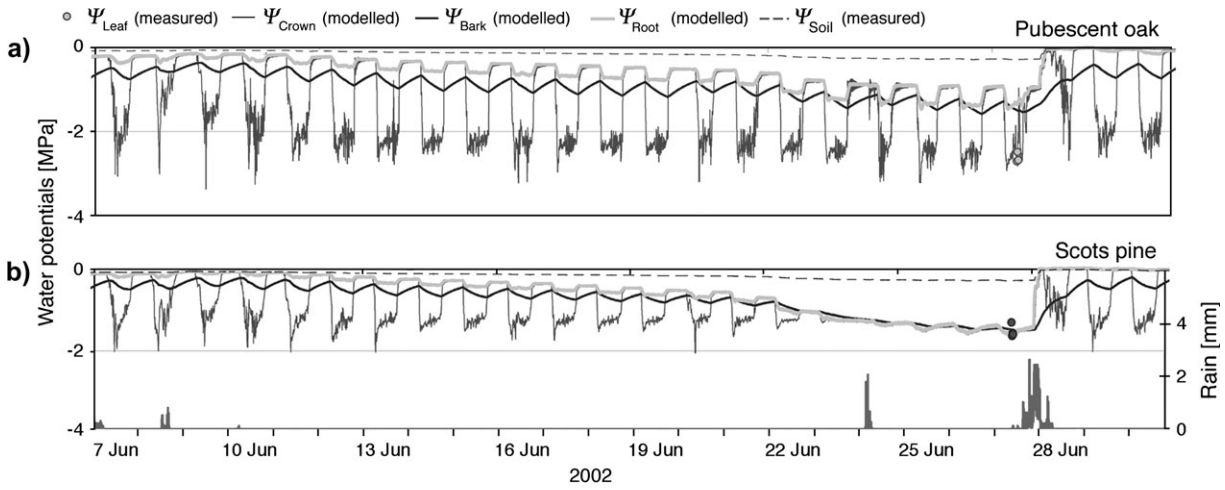

Fig. 8. Courses of water potentials in soil (Ψ_{Soil}), roots (Ψ_{Root}), bark (Ψ_{Bark}), and crown (Ψ_{Crown}) of (a) Pubescent oak and (b) Scots pine during a drought period in June 2002 (see also Fig. 3). Rain at the site is quantified on the right axis of (b).

In general, oak reached slightly lower root water potentials than pine (Table 3). By contrast, pine seemed to reach a critical predawn water potential level at about –1.5 MPa (22–27 June, Fig. 8). The coniferous species was hardly able to keep its stomata open (Fig. 3), thus, the water potentials within the trees levelled off, the corresponding potential gradients disappeared and no water transport could be maintained. After the rain at 28 June 2002 (Figs 3, 8), both species returned to physiological patterns that were observed before the drought started.

Sensitivity of the (model) stomata: species-specific patterns

According to equation 3, the effect of light on θ is determined by *Rad*, Γ_{Rad}, and Φ_{Rad}. Darkness leads to a closing signal whereas light induces an opening signal (Fig. 9). Both species reached the signal towards opening stomata at relatively low *Rad* (pine <50 W m^{-2}, oak <100 W m^{-2}). The model successfully determined the timing of stomatal opening in the morning and stomatal closure in the evening (equation 3). This stomatal response to radiation may be a simplification and did, for instance, not allow for possible night-time transpiration. This approach, however, facilitated the analysis of the effects of water potential and tree water deficit on physiological patterns between sunrise and sunset.

The course of Ψ_{Crown} was mainly responsible for the diurnal course of θ during daylight (Fig. 9). But because of the combination of the different (opposing) signals, the response of θ to Ψ_{Crown} was non-linear and resulted in hysteresis between these two factors within day courses (Fig. 10).

The signal of ΔW on θ was found to be stomata closing for pine and stomata opening for oak (Table 2). This means that with increasing drought stress the stomata of oak tended to stay open longer at a given decrease of Ψ_{Crown}, whereas the stomata of pine tended to close faster under the same microclimatic conditions (Fig. 9). The stomatal responses of oak and pine thus diverged under contrasting conditions: by contrast with oak, pine had a less intensive closure of the stomata during the wet

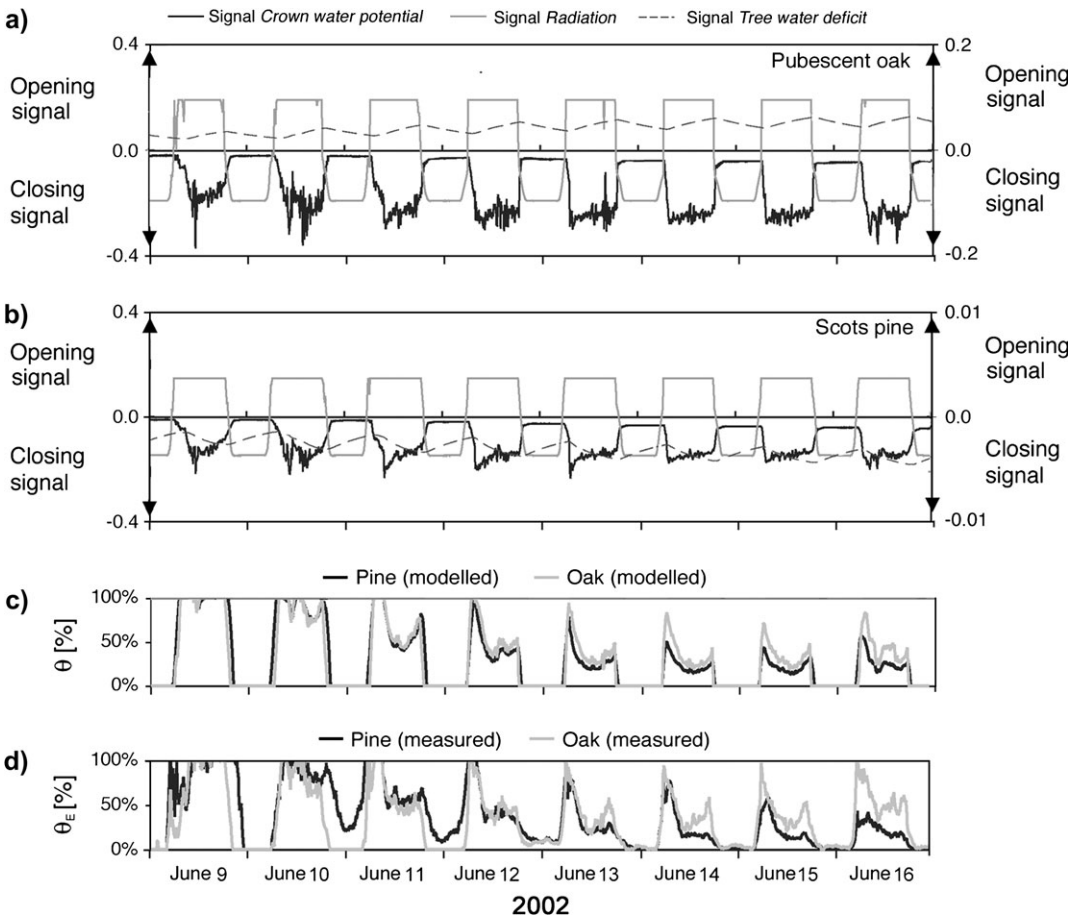

Fig. 9. Signals of light (left *y*-axis), crown water potential (left *y*-axis) and tree water deficit (right *y*-axis) (equation 3) affecting stomatal regulation over a drying period in June 2002 (see also Fig. 3). (a) Pubescent oak. (b) Scots pine. (c) Modelled relative stomatal closure (θ), and (d) measured relative stomatal closure of the two species (θ_E). Related crown water potentials are shown in Fig. 8.

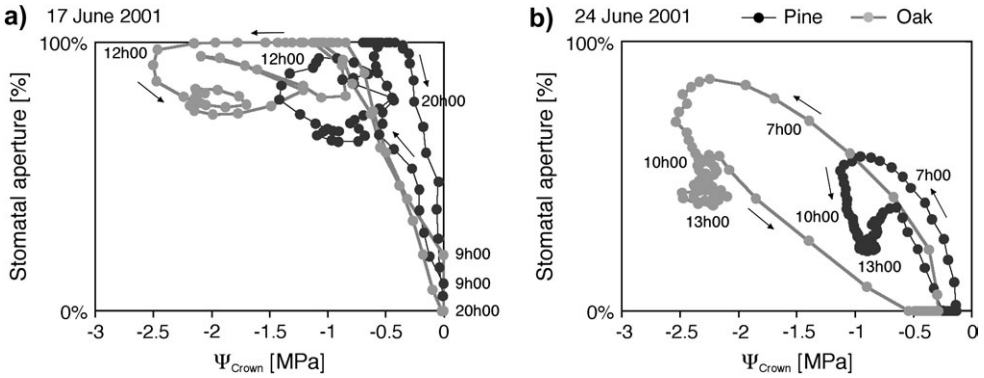

Fig. 10. Modelled hysteresis patterns of Pubescent oak (grey symbols) and Scots pine (black symbols). Crown water potential (Ψ_{Crown}) in relation to the stomatal aperture on two days in the drying period in June 2001. (a) 17 June 2001 (wet). (b) 24 June 2001 (dry). Every dot represents a 10 min value. Arrows indicate the time course, numbers refer to daytime.

conditions, but a stronger closure the drier the conditions became. Eight days without rain in June 2002 (Fig. 9) are a good example for the divergently developing responses to drought of the two species. The different responses became also visible on 24 June 2001 (Fig. 10), when stomatal aperture of pine was much more reduced than that of oak.

Discussion

Three steps from data to modelling and interpretation

Temporally highly resolved ecophysiological field data of Scots pine and Pubescent oak over three years were analysed in three steps: (i) a pattern analysis to recognize species-specific responses to microclimate, (ii) a model simulation to quantify the goodness-of-fit of the new model approach, and (iii) an interpretation of model assumptions and parameters to explain the species-specific differences with mechanisms and plant properties:

(i) From the analysis of measured data it was learned that pine kept its stomata more open than oak under relatively humid conditions, but closed stomata more rapidly and maintained higher crown water potentials with increasing drought. Since it was suggested that these trees had no or only little access to deeper water sources via cracks in the rock (Zweifel *et al*., 2005), the observed difference in the responses between oak and pine are considered to be mostly physiologically, and not environmentally, driven. (ii) The model with a mechanistic backbone for tree water relations and empirically weighted feedback loops to the stomata (Fig. 1) successfully predicted the species-specific stomatal response patterns on a diurnal and seasonal time-scale, as well as for successive years. While in most other models (Ball *et al*., 1987; Leuning, 1990; Tuzet *et al*., 2003; Xu and Baldocchi, 2003) empirical response functions predefined the relationships between stomatal sensitivity and, for example, leaf water potential, such relationships emerge from the model assumptions on integrated water relations, feedback signals, and the species-specific parameterization in our modelling approach. (iii) The quality of simulation was high enough to interpret the model assumptions and the optimized parameters for physiological information. The species-specific model tree properties suggested that oak had higher flow resistances than pine and that it withdrew more water from the storage pools than its coniferous neighbour. These properties and the species-specific stomatal sensitivity, particularly to tree water deficit, led to a consistent explanation for the observed ecophysiological measurements.

Model parameters

Three of the optimized parameters of the model which could be compared to values reported in literature were the hydraulic resistances of the flow path (R_1, R_3) and the water storage capacitance of stem (C_{Stem}) and crown (C_{Crown}). The obtained hydraulic flow resistances were between 0.00021 and 0.01394 MPa h g^{-1}. The values are within the lower end of the range of hydraulic resistances in tree species reported in literature, ranging between 0.00028 and 0.051 MPa h g^{-1} (Steppe, 2004). The values for C_{Stem} (ranging from 78–269 g MPa^{-1}) and C_{Crown} (ranging from 86–222 g MPa^{-1}) were also found to be within the wide range of values reported, varying from 0.2–1440 g MPa^{-1} (Hunt *et al*., 1991; Kobayashi and Tanaka, 2001; Steppe, 2004; Steppe *et al*., 2006). Yet, the values cited are to be handled with care when comparing them with the ones obtained in this investigation since they refer in no case to mature trees under similarly dry field conditions. The trees cited were younger (Steppe, 2004), potted (Steppe, 2004) or growing under moderate wet conditions (Hunt *et al*., 1991). This may at least partially explain the variety of parameter values found.

Diverging response of pine and oak to tree water deficit

Pubescent oak had higher flow resistances and lower minimum crown water potentials (–4.8 MPa versus –2 MPa)

than Scots pine (Figs 6–8; Table 3). As radial exchange resistance (R_2) did not differ significantly between both species, these more negative water potentials enabled oak to withdraw more water from the leaves compared with pine, despite its lower hydraulic crown water capacitance (Table 2).

Yet, the most striking difference between the two species occurred in the signal from tree water deficit to the stomata. The stomata of pine showed a more sensitive response to increasing drought because both the tree water deficit and the crown water potential had a closing effect (Fig. 9). By contrast, the stomata of oak became less sensitive with increasing drought as the closing effect of the rapidly changing crown water potential was opposed by an opening effect of the slowly changing tree water deficit (Fig. 9). These species-specific differences in properties led to relatively more open stomata of pine during relatively wet conditions (Ψ_{Soil} > approximately –50 kPa) and to relatively more open stomata of oak during dry conditions (Ψ_{Soil} < approximately –50 kPa). Consequently, oak had an advantage over pine in dry conditions in terms of keeping its stomata open and thus a potential advantage in fixing CO_2 with photosynthesis. These results further suggest that oak was more efficient in water uptake than pine during dry periods. The lower root water potentials predicted by the model for oak, compared with pine (Table 3), support this finding and suggest a competitive advantage of root water uptake of oak over pine during drought periods.

Diurnal patterns

The tree model assumes that the diurnal regulation of stomatal aperture depends on signals from light, the current stomatal aperture, crown water potential, and tree water deficit (equation 3). Light delivers a strong signal that initiates a rapid opening of stomata in the morning twilight, and a rapid closing of stomata in the evening (Fig. 9). The signal from crown water potential opposes the opening signal from light during the day. This signal may slow down the opening of stomata in the morning, and provoke a midday depression (Xu and Shen, 1997) or gradual closure of stomata during the day. Although the signal from tree water deficit was relatively small (Fig. 9), it had significant effects on the diurnal patterns of stomatal aperture, particularly under dry conditions (see section 'seasonal patterns').

The importance of this tree water deficit can be illustrated by comparing the stomatal aperture against crown water potential on a dry versus a wet day (Fig. 10). The hysteresis is particularly strong on a dry day (Takagi *et al*., 1998; Oren *et al*., 2001; Tuzet *et al*., 2003). Tuzet *et al*. (2003) suggested that the diurnal changes in soil and root water potential may explain this pattern. Our model results suggest an alternative, or additive, contribution of the hydraulic system to hysteresis in the stomatal aperture, via the diurnal changes in water storage and its consequences for the signals from the tree water deficit and, indirectly, from the crown water potential.

Seasonal patterns

The tree model successfully predicted the differences in the physiological dynamics between Scots pine and Pubescent oak during ongoing drought. Pines had lower hydraulic resistances, lower water consumption and, on average, less negative leaf and root water potentials than oak (Tables 2, 3). In pine, the minimum leaf water potentials tended to go towards less negative values, and stomatal aperture and transpiration gradually decreased as the soil dried (Figs 8, 9). The decrease in the water potential gradient between crown and roots and the decreasing stomatal aperture is attributed to the sum of the closing signals by crown water potential and tree water deficit, whereby the tree water deficit signal became more important while the soil dried. By contrast, oak maintained the minimum crown water potential at an almost constant level (Fig. 8). In this species, a closing signal by crown water potential was partially compensated by an opening signal of tree water deficit, which increased with ongoing drought. The interaction between these two opposing signals and the hydraulic properties may explain why oaks remained physiologically active over longer periods than pines during drought periods. We can thus conclude that the same signalling responses, as driven by the hydraulic system, explain the physiological divergence between the pine and oak on diurnal and seasonal time scales.

Heat wave in 2003

During the extreme drought in 2003 (Beniston, 2004), Pubescent oak and Scots pine (like other tree species in this area) dramatically reduced their physiological activity from mid-July onwards (Zweifel *et al*., 2006). The leaves of oak either turned white from one day to the next or they showed early leaf senescence like that usually observed in autumn. During the same period pine had more needles than usual that turned yellowish and were shed about one month later. We may speculate that the roots were no longer able to supply sufficient water to the tree body to maintain a balance between saving water to avoid cavitation and transpiring water to cool overheated leaves. Although we are uncertain whether the leaves wilted because of heat damage or embolized elements in the water supply chain, the early loss of leaves might have helped to avoid lethal damage to the conducting system of individual branches or even of the main water-conducting system of the stem.

The hydraulic resistances (model result) in the second half of 2003 were found to be markedly increased compared with the two previous years (Table 2). This increase can be attributed to cavitation occurring more intensely in dry periods (corresponding to acoustic emission data, data

not shown). As many investigations suggested, cavitation increases the hydraulic resistance in the flow path of trees because every event reduces the conducting area of the xylem (Grace, 1993; Sperry *et al.*, 1993; Magnani and Borghetti, 1995; Vilagrosa *et al.*, 2003).

Conclusions

The investigation gives an explanation of how soil water potential, microclimate, and the hydraulic system, including water transport and storage, influence stomatal aperture and transpiration in Scots pine and Pubescent oak during three successive growth seasons.

The model predictions revealed diverging species-specific dynamics in gas exchange which were caused by differences in physiological properties. The properties of Pubescent oak with a higher hydraulic flow resistance, the ability to withdraw larger amounts of stored water from stem and crown, and the ability to maintain lower water potentials from the leaves to the roots without inducing cavitation, led to relatively more opened stomata during dry conditions compared with pine.

The model assumptions did not allow for predicting night time transpiration (Phillips and Daley, 2006) and revealed a dynamic in hydraulic resistances over time, which were assumed to be constant in the model. Nevertheless, the model successfully predicted multiple patterns related to stomatal aperture, while for example the leaf CO_2 concentration was not considered (Farquhar and Wong, 1984).

The species-specific differences in functional properties are concluded to be the reason for a more efficient water uptake from dry soil and thus a competitive advantage of Pubescent oak over Scots pine in an environment which has been exposed to increasing temperatures and more frequent droughts over the past decades (Beniston, 2004). Our results from the extreme drought year 2003, however, suggest that both pine and oak completely ceased their physiological activity, and emphasize the potentially serious consequences of ongoing climate change for both pines and oaks in this area.

Acknowledgements

We are grateful to DM Newbery of the Institute of Plant Sciences of the University of Bern for supporting the field work in the Wallis. We thank E Bhend for the great support with the set up and maintenance of the research stations and we appreciate the conceptual inputs and practical help in the field of L Zimmermann and M Lingenfelder. We are indebted to Fabienne Zeugin, Sara Bangerter, Marijn Swart, Simone de Brock, and Alfred Chitiki for their fieldwork at Salgesch.

The research was part of the project 'Tree Response to Climate Change', supported by a Swiss Federal Research Fellowship for Roman Zweifel and additionally funded by the Swiss National Science Foundation, project 'Thermoak in NCCR, Climate', the Institute of Plant Sciences of the University of Bern, and the Swiss Federal Institute for Forest, Snow and Landscape Research (WSL), Birmensdorf. Frank Sterck was financially supported by the SBP foundation of KNAW. Kathy Steppe was financially supported as a Postdoctoral Fellow of the Research Foundation – Flanders (FWO).

Appendix A list of parameters

	Unit	Description	Measured Calculated Optimized	Model-Input Model-Output Constant	Scaled/interpolated[a]
Microclimate					
Rad	[W m^{-2}]	Net radiation	Measured	Input/Input eq. 1	Interpolated for crown expositions
PAR	[μmol m^{-2} s^{-1}]	Photosynthetic active radiation	Measured	Input eq. 1	Interpolated
T	[°C]	Air temperature	Measured	Input eq. 1	Interpolated
Rain	[mm]	Rain	Measured		
RH	[%]	Relative humidity of air	Measured		
VPD	[kPa]	Vapour pressure deficit of air	Calculated from *T* and *RH*	Input eq. 1	Interpolated
u_z	[m s^{-1}]	Wind speed	Measured	Input eq. 1	
Ψ_{Soil}	[kPa]	Soil water potential	Measured	Input	Interpolated
Potential transpiration					
F_{Pot_Branch}	[g h^{-1}]	Potential transpiration for a branch-like geometric surface with constant porosity	Calculated from microclimate and F_{Branch}[b], eq. 1		
F_{Pot}	[g h^{-1}]	Potential transpiration of a crown	Calculated	Input	Scaled up to crown size from
r_a	[s m^2 m^{-3}]	Aerodynamic boundary layer resistance of branch	Calculated[b], eq. 2	Output	
Δs	[ ]	Slope of the saturation vapour pressure curve	Calculated[b], eq. 2	Output	
χ	[ ]	Proportion of direct solar irradiation and shaded parts of the crown	Optimized[b] for eq. 2	Constant	

Appendix A (*Continued*)

	Unit	Description	Measured Calculated Optimized	Model-Input Model-Output Constant	Scaled/interpolated[a]
		(χ=0.01: branch completely shaded; χ=0.5: branch completely in the sun)			
W_H	[MJ kg^{-1} °K^{-1}]	Heat flux between stem and branch. W_H= 0		Constant	
ρ	[kg m^{-3}]	Air density	Calculated, eq. 2,	Output	
c_p	[MJ kg^{-1} °K^{-1}]	Specific heat of the air (1.01 * 10^{-3})		Constant	
γ	[kPa °K^{-1}]	Psychrometer coefficient	Calculated[b], eq. 2	Output	
δ	[m]	Boundary layer thickness of the branch surface	Calculated[b], eq. 2	Output	
Z_T	[m^2]	Idealized branch surface	Optimized[b] for eq. 2	Constant	
$r_{s\ min}$	[s m^2 m^{-3}]	Minimum stomatal resistance of the branch	Optimized[b] for eq. 2	Constant	
λ	[MJ kg^{-1}]	Latent heat of vaporization of water	Calculated[b], eq. 2	Output	
Tree					
F_{Branch}	[g h^{-1}]	Branch sap flow rates	Measured		Scaled up to tree size. (1)
F_1	[g h^{-1}]	Water flow through root and lower stem section	Calculated, Appendix B	Output	
F_2	[g h^{-1}]	Water flow into and out of the stem storage tissues	Calculated, Appendix B	Output	
F_3	[g h^{-1}]	Water flow through upper stem section towards the crown	Calculated, Appendix B	Output	
F_{Transp}	[g h^{-1}]	Transpiration	Calculated, eq. 1	Output	(1)
Ψ_{Root}	[MPa]	Root water potential	Calculated, = Ψ_{SoilR}	Output	
Ψ_{Bark}	[MPa]	Bark water potential	Calculated, eq. B6	Output	
Ψ_{Crown}	[MPa]	Crown water potential	Calculated, eq. B7	Output	(2)
Ψ_{Leaf}	[MPa]	Leaf water potential	Measured		Interpolated for crown expositions (2)
R_1	[h g^{-1}]	Flow resistance root/stem	Optimized	Constant	
R_2	[h g^{-1}]	Flow resistance stem/bark	Optimized	Constant	
R_3	[h g^{-1}]	Flow resistance stem/crown=R_1	=R_1	Constant	
P_{Stem}	[g]	Tree water storage	Calculated, eq. B5	Output	(3)
$P_{Stem\ max}$	[g]	Maximum available water from the bark=800	Set	Constant	
P_{Crown}	[g]	Crown water storage	Calculated, eq. B4	Output	
$P_{Crown\ max}$	[g]	Maximum available water from the crown=5000	Set	Constant	
ΔR	[μm]	Stem radius changes	Measured		
ΔW	[μm]	Tree water deficit	Calculated from ΔR, (Zweifel *et al*., 2005)		(3)
θ_{e_Branch}	[]	Estimated stomatal aperture of a branch	Measured and calculated from F_{Branch} and F_{Pot}		
θ_e	[]	Scaled up estimated stomatal aperture of the crown	Calculated from θ_{e_Branch}		Scaled up to tree size (4)
θ	[]	Modelled stomatal aperture of the crown	Calculated, eq. 3	Output	(4)
Φ_{Crown}	[MPa^{-1}]	Weighting-factor for the impact of Ψ_{Crown} on θ=0.11	Set	Constant	
Φ_{Bark}	[g^{-1}]	Weighting-factor for the impact of ΔW on θ	Optimized	Constant	
Φ_{Rad}	[ ]	Weighting-factor for the impact of *Rad* on θ	Optimized	Constant	
Γ_{Rad}	[W m^{-2}]	Threshold for light (impact on θ)	Optimized	Constant	
C_{Crown}	[g MPa^{-1}]	Crown water capacitance	Optimized	Constant	
C_{Stem}	[g MPa^{-1}]	Stem water capacitance	Optimized	Constant	
k_1	[ ]	Transformation factor 1 for calculating Ψ_{Root} from Ψ_{Soil}	Optimized	Constant	
k_2	[ ]	Transformation factor 2 for calculating Ψ_{Root} from Ψ_{Soil}	Optimized	Constant	

[a] Numbers in brackets indicate the pair of variables which were compared between measurement and model output.
[b] (Zweifel *et al*., 2002).

Appendix B: equations of the flow and storage system

The flow and storage concept of this model is based on the water flow along water potential gradients, corresponding to the dynamically changing water potentials in roots (Ψ_{Roots}), bark (Ψ_{Bark}), and crown (Ψ_{Crown}). This concept can be understood as a hydraulic system (Fig. 1a) whose flow dynamics between given water potential poles are analogous to the electron flow in an electrical circuit. The main driving force for water fluxes is the current transpiration (F_{Transp}). Due to the water loss from the crown by F_{Transp}, crown water potential (Ψ_{Crown}) decreases and water potential gradients are induced between the crown and the bark (Ψ_{Bark}), roots (Ψ_{Roots}), and soil (Ψ_{Soil}). Along these gradients water is transported in the xylem from roots, through the stem and branches to the bark and the leaves (F_1, F_2, and F_3), according to the cohesion theory. Two water storage compartments are located in the flow system of this model tree: the stem (P_{Stem}) and the crown (P_{Crown}). The stem water storage mainly consists of water in the elastic phloem cells in the bark and of available water in the wood. Crown water storage consists of water in the elastic cells of the crown mainly in the leaves. Both compartments are coupled to the hydraulic system and thus stem and crown become depleted or replenished depending on the occurring pattern of water potentials. The depletion of the bark becomes visible in a shrinkage of the stem. If F_{Transp} stops and Ψ_{Soil} remains unchanged the fluxes level out the gradients within the tree and water movement ceases. Hydraulic flow resistances are applied for the two stem segments (R_1 and R_3) and for the water exchange between the xylem and the stem water storage compartments (R_2).

For given water potential values and flow resistances (R_1 to R_3), the resulting water movement in the lower (F_1) and upper stem section (F_3), and the water exchange between xylem and tree water storage (F_2) can be calculated. The flow equations are obtained by applying Kirchhoff's current law to the junctions and nodes in the circuit, whereby the flow rates are assumed to be analogue to the traditional currents in an electrical network according to the Ohm's law. Equations B1 to B3 formulate the flow rates for F_1, F_2, and F_3 (Zweifel *et al*., 2001; Steppe *et al*., 2006):

$$F_1 = F_2 + F_3 \tag{B1}$$

$$F_3 = \frac{\Psi_{Bark} - \Psi_{Crown} + F_2 R_2}{R_3} \tag{B2}$$

$$F_2 = \frac{\Psi_{Root} R_3 - \Psi_{Bark} R_3 - \Psi_{Bark} R_1 + \Psi_{Crown} R_1}{R_2 R_3 + R_1 R_3 + R_2 R_1} \tag{B3}$$

Transpiration (F_{Transp}) and the water flow in and out of storage locations changes the hydration status of stem (P_{Stem}) and crown (P_{Crown}):

$$P_{Crown,t=i} = P_{Crown,t=i-1} - F_{Transp} \times \Delta_t + F_3 \times \Delta_t \tag{B4}$$

$$P_{Stem,t=1} = P_{Stem,t=i-1} + F_2 \times \Delta_t \tag{B5}$$

To link the flow equations (B1 to B3) to the storage status of the tree (equations B4 and B5), P_{Stem} and P_{Crown} have to be set in relation to the water potential of the respective compartment. From a given water status of a storage compartment, the water potential can be calculated as:

$$\Psi_{Bark} = \frac{P_{Stem} - P_{Stem\,max}}{C_{Stem}} = \frac{\Delta P_{Stem}}{C_{Stem}} \tag{B6}$$

$$\Psi_{Crown} = \frac{P_{Crown} - P_{Crown\,max}}{C_{Crown}} \tag{B7}$$

where $P_{Stem\ max}$ is the maximally available water that can be withdrawn from the elastic stem tissues (mainly the bark), ΔP_{Stem} is (negative) stem water deficit which is assumed to be proportional to (positive) tree water deficit (ΔW)(Zweifel *et al*., 2005), $P_{Crown\ max}$ is maximally available water that can be withdrawn from the leaves, and C_{Stem} and C_{Crown} are capacitances of the respective storage (Steppe, 2004; Steppe *et al*., 2006). The (constant) capacitances determine how much water is withdrawn from the storage compartment for a given change in water potential and how P_{Crown} is related to Ψ_{Crown}: the lower P_{Crown} is the more negative is Ψ_{Crown}.

Equation for the soil water and root conditions

Several investigations showed that measured mean soil matric water potential (Ψ_{Soil}) is more moderate than the conditions in the soil next to the roots (Donovan *et al*., 2001; Mediavilla and Escudero, 2003; Tuzet *et al*., 2003). Tuzet *et al*. (2003) found that the variation in Ψ_{Soil} is a function of distance from the roots and concluded that the use of Ψ_{Soil} as a measure for root water potential (Ψ_{Root}) leads to incorrect values of resistances to plant water flow especially during periods of drying soil. The non-linear decrease of water potentials between a point at a certain distance to the roots and the soil next to the roots is functionally explainable with an increasing resistance to water flow in drying soil accelerated by the root water uptake. The relationship can be formulated as:

$$\Psi_{Root} = k_1 (F_{1(2h)}) \mathrm{abs}(\Psi_{Soil})^{k_2} \tag{B8}$$

where Ψ_{Root} is assumed to be equal to the soil water potential next to the root surface, $F_{1(2h)}$ is the mean root water uptake of the past 2 h and k_1 and k_2 are soil and plant specific parameters of the model.

Appendix C: sensitivity analysis

Sensitivity analysis

The sensitivity analysis covered two aspects: (i) the model sensitivity on variations of the parameters to select the parameters driving most of the variability in the model outputs and (ii) the degree of independency of individual parameters to test whether pairs of parameters were compensating each other.

(a) The model sensitivity $S(\bar{y}_i)$ on each parameter was calculated according to Steppe *et al*. (2006) as:

$$S(\bar{y}_i) = \frac{\bar{y}_i(\tau + \Delta\tau) - \bar{y}_i(\tau - \Delta\tau)}{2 \times \bar{y}_i(\tau)} 100 \tag{C1}$$

where $\bar{y}_i(\tau)$ is the model output at the time i with the original parameter value τ and the perturbation $\Delta\tau$. Perturbation was chosen to be 10% of τ. Based on $S(\bar{y}_i)$, the sensitivity measure ξ^{meas} was calculated as:

$$\xi^{meas} = \frac{1}{N} \sum_{i=1}^{N} \left| S(\bar{y}_i) \right| \tag{C2}$$

where N is the number of $S(\bar{y}_i)$-values along the time axis. A high ξ^{meas} for a certain parameter means a high sensitivity of the model on this parameter. A ξ^{meas} close to zero means that the model does not depend on this parameter very strongly.

(b) The dependency of pairs of parameters were tested with a correlation of the respective $S(\bar{y}_i)$-values. If a parameter was found to be highly correlated to others, it was set and not involved into the parameterization process.

The sensitivity analysis was done with 10 of the 13 model parameters. Three parameters were pre-set: R_3, $P_{\text{Crown max}}$, and $P_{\text{Stem max}}$. The flow resistances for the upper stem section R_3 was set equal to R_1. There was no reason to deal with different resistances because the stem storage was reduced to a single spot in the middle of the flow path and the model is therefore not able to differentiate between small variations in resistances along the flow path. $P_{\text{Crown max}}$ was set to 5000 g. This value was roughly estimated from values in literature for other tree species (Hunt *et al*., 1991; Zweifel and Häsler, 2001; Steppe, 2004). A good estimate for $P_{\text{Crown max}}$ was to take 1.5-fold the value of the maximally measured stem sap flow rate (g h^{-1}) as a maximum value of water storage (g). Similar reflections led to the setting of $P_{\text{Stem max}}$=800 g, which was about a quarter of the maximally measured stem sap flow rate.

The averaged sensitivities of the model outputs F_1, ΔW, Ψ_{Crown}, and θ on the 10 parameters were ranked as follows: k_2=R_1 >C_{Crown} >Φ_{Crown}=Φ_{Bark} >C_{Stem} >k_1=Φ_{Rad} >Γ_{Rad} >R_2. Slightly changed rankings occurred with different parameterizations. Overall, F_1 was found to be most sensitive on parameter perturbations in comparison to ΔW, Ψ_{Crown}, and θ. High correlations were found between the parameters Φ_{Crown} and Φ_{Bark}, Φ_{Crown}, and C_{Stem}, and Φ_{Bark} and C_{Stem}. These findings led to the exclusion of Φ_{Crown} from the parameterization process. The parameter Φ_{Crown} was set to the constant value of 0.11, which was about the average within the range of values obtained in about 100 model test runs. The other nine parameters were identifiable with the parameterization procedure.

References

Ball JT, Woodrow IE, Berry JA. 1987. A model predicting stomatal conductance and its contribution to the control of photosynthesis under different environmental conditions. In: Biggins J, ed. *Progress in photosynthesis*. Dordrecht: Martinus Nijhoff, 221–224.

Beniston M. 2004. The 2003 heat wave in Europe: A shape of things to come? *Geophysical Research Letters* 31, L02202.

Bond BJ, Kavanagh KL. 1999. Stomatal behavior of four woody species in relation to leaf-specific hydraulic conductance and threshold water potential. *Tree Physiology* **19,** 503–510.

Brodribb TJ, Holbrook NM. 2003. Stomatal closure during leaf dehydration, correlation with other leaf physiological traits. *Plant Physiology* **132,** 2166–2173.

Buckley TN. 2005. The control of stomata by water balance. *New Phytologist* **168,** 275–292.

Buckley TN, Mott KA, Farquhar GD. 2003. A hydromechanical and biochemical model of stomatal conductance. *Plant, Cell and Environment* **26,** 1767–1785.

Comstock J, Mencuccini M. 1998. Control of stomatal conductance by leaf water potential in *Hymenoclea salsola* (T.&G.), a desert shrub. *Plant, Cell and Environment* **21,** 1029–1038.

Daudet FA, Ameglio T, Cochard H, Archilla O, Lacointe A. 2005. Experimental analysis of the role of water and carbon in tree stem diameter variations. *Journal of Experimental Botany* **56,** 135–144.

Davies WJ, Zhang J. 1991. Root signals and the regulation of growth and development of plants in drying soil. *Annual Review of Plant Physiology* **42,** 55–76.

Dewar RC. 2002. The Ball–Berry–Leuning and Tardieu–Davies models: synthesis and extension at guard cell level. *Plant, Cell and Environment* **19,** 1383–1398.

Dixon HH, Joly J. 1894. On the ascent of sap. *Philosophical Transactions of the Royal Society of London B, Biological Sciences* **186,** 563–576.

Dodd IC. 2003. Hormonal interactions and stomatal responses. *Journal of Plant Growth Regulation* **22,** 32–46.

Donovan LA, Linton MJ, Richards JH. 2001. Predawn plant water potential does not necessarily equilibrate with soil water potential under well-watered conditions. *Oecologia* **129,** 328–335.

Eisinger WR, Bogomolni RA, Taiz L. 2003. Interactions between a blue-green reversible photoreceptor and a separate UV-B receptor in stomatal guard cells. *American Journal of Botany* **90,** 1560–1566.

Farquhar GD, Wong SC. 1984. An empirical model of stomatal conductance. *Australian Journal of Plant Physiology* **11,** 191–210.

Grace J. 1993. Refilling of embolized xylem. In: Borghetti M, Grace J, Raschi A, eds. *Water transport in plants under climatic stress*. Cambridge: Cambridge University Press, 52–62.

Hanson PJ, Amthor JS, Wullschleger SD, *et al*. 2004. Oak forest carbon and water simulations: model intercomparisons and evaluations against independent data. *Ecological Monographs* **73,** 443–489.

Hinckley TM, Lassoie JP. 1981. Radial growth in conifers and deciduous trees: a comparison. *Mitteilungen der forstlichen Bundesversuchsanstalt Wien* **142,** 17–56.

Hsiao TC, Acevedo E. 1974. Plant responses to water deficits, water-use efficiency, and drought resistance. *Agricultural Meteorology* **14,** 59–84.

Hunt R, Running SW, Federer CA. 1991. Extrapolating plant water flow resistances and capacitances to regional scales. *Agricultural and Forest Meteorology* **54,** 169–195.

Kobayashi Y, Tanaka T. 2001. Water flow and hydraulic characteristics of Japanese red pine and oak trees. *Hydrological Processes* **15,** 1731–1750.

Larcher W. 2003. *Physiological plant ecology. Ecophysiology and stress physiology of functional groups*, 4th edn. Springer, Berlin.

Leuning R. 1990. Modeling stomatal behavior and photosynthesis of *Eucalyptus grandis*. *Australian Journal of Plant Physiology* **17,** 159–175.

Leuning R. 1995. A critical appraisal of a combined stomatal-photosynthesis model for C-3 plants. *Plant, Cell and Environment* **18,** 339–355.

Magnani F, Borghetti M. 1995. Interpretation of seasonal changes of xylem embolism and plant hydraulic resistance in *Fagus sylvatica*. *Plant, Cell and Environment* **18,** 689–696.

Mayer DG, Butler DG. 1993. Statistical validation. *Ecological Modelling* **68,** 21–32.

Mediavilla S, Escudero A. 2003. Stomatal responses to drought at a Mediterranean site: a comparative study of co-occurring woody species differing in leaf longevity. *Tree Physiology* **23,** 987–996.

Meinzer FC, Andrade JL, Goldstein G, Holbrook NM, Cavelier J, Jackson P. 1997. Control of transpiration from the upper canopy of a tropical forest: the role of stomatal, boundary layer and hydraulic architecture components. *Plant, Cell and Environment* **20,** 1242–1252.

Messinger SM, Buckley TN, Mott KA. 2006. Evidence for involvement of photosynthetic processes in the stomatal response to CO_2. *Plant Physiology* **140,** 771–778.

Monteith JL. 1965. Evaporation and environment. *Symposium of the Society of Experimental Biology* **19,** 205–234.

Oren R, Sperry JS, Ewers BE, Pataki DE, Phillips N, Megonigal JP. 2001. Sensitivity of mean canopy stomatal conductance to vapour pressure deficit in a flooded *Taxodium distichum* L. forest: hydraulic and non-hydraulic effect. *Oecologia* **126,** 21–29.

Penman HL. 1948. Natural evaporation from open water, bare soil and grass. *Proceedings of the Royal Society of London* **193,** 120–146.

Perämäki M, Nikinmaa E, Sevanto S, Ilvesniemi H, Siivola E, Hari P, Vesala T. 2001. Tree stem diameter variations and transpiration in Scots pine: an analysis using a dynamic sap flow model. *Tree Physiology* **21,** 889–897.

Phillips NG, Daley MJ. 2006. Interspecific variation in night-time transpiration and stomatal conductance in a mixed New England deciduous forest. *Tree Physiology* **26,** 411–419.

Reynolds MR. 1984. Estimating the error in model predictions. *Forest Sciences* **30,** 454–469.

Sperry JS. 2003. Evolution of water transport and xylem structure. *International Journal of Plant Sciences* **164,** S115–S127.

Sperry JS, Alder NN, Eastlack SE. 1993. The effect of reduced hydraulic conductance on stomatal conductance and xylem cavitation. *Journal of Experimental Botany* **44,** 1975–1982.

Sperry JS, Hacke UG, Oren R, Comstock JP. 2002. Water deficits and hydraulic limits to leaf water supply. *Plant, Cell and Environment* **25,** 251–263.

Steppe K. 2004. Diurnal dynamics of water flow through trees: design and validation of a mathematical flow and storage model. PhD thesis, University of Gent, Gent.

Steppe K, De Pauw DJW, Lemeur R, Vanrolleghem PA. 2006. A mathematical model linking tree sap flow dynamics to daily stem diameter fluctuations and radial stem growth. *Tree Physiology* **26,** 257–273.

Takagi K, Tsuboya T, Takahashi H. 1998. Diurnal hystereses of stomatal and bulk surface conductance in relation to water vapour pressure deficit in cool-temperate wetland. *Agricultural and Forest Meteorology* **91,** 177–191.

Tardieu F, Davies WJ. 1993. Integration of hydraulic and chemical signalling in the control of stomatal conductance and water status of droughted plants. *Plant, Cell and Environment* **16,** 341–349.

Tenhunen JD, Pearcy RW, Lange OL. 1987. Diurnal variations in leaf conductance and gas exchange in natural environment. In: Zeiger E, Farquhar GD, Cowan IR, eds. *Stomatal function*. Stanford: Stanford University Press, 323–351.

Thompson MV, Holbrook NM. 2004. Scaling phloem transport: information transmission. *Plant, Cell and Environment* **27,** 509–519.

Tuzet A, Perrier A, Leuning R. 2003. A coupled model of stomatal conductance, photosynthesis and transpiration. *Plant, Cell and Environment* **26,** 1097–1116.

Tyree MT. 1988. A dynamic model for water flow in a single tree: evidence that models must account for hydraulic architecture. *Tree Physiology* **4,** 195–217.

Tyree MT, Sperry JS. 1989. Vulnerability of xylem to cavitation and embolism. *Annual Review of Plant Physiology and Plant Molecular Biology* **40,** 19–38.

van den Honert TH. 1948. Water transport in plants as a caternary process. *Faraday Society Discussions* **3,** 146–153.

Vilagrosa A, Bellot J, Vallejo VR, Gil-Pelegrin E. 2003. Cavitation, stomatal conductance, and leaf dieback in seedlings of two co-occurring Mediterranean shrubs during an intense drought. *Journal of Experimental Botany* **54,** 2015–2024.

Walters DK. 1994. Evaluation methodology for forest ecosystem change models. PhD thesis. University of Minnesota, USA.

Whitehead D. 1998. Regulation of stomatal conductance and transpiration in forest canopies. *Tree Physiology* **18,** 633–644.

Wright IJ, Reich PB, Westoby M. 2003. Least-cost input mixtures of water and nitrogen for photosynthesis. *American Naturalist* **161,** 98–111.

Xu DQ, Shen YK. 1997. Midday depression of photosynthesis. In: Pessarakli M, ed. *Handbook of photosynthesis*. New York: Marcel Dekker, Inc., 451–459.

Xu LK, Baldocchi DD. 2003. Seasonal trends in photosynthetic parameters and stomatal conductance of blue oak (*Quercus douglasii*) under prolonged summer drought and high temperature. *Tree Physiology* **23,** 865–877.

Zweifel R, Böhm JP, Häsler R. 2002. Midday stomatal closure in Norway spruce: reactions in the upper and lower crown. *Tree Physiology* **22,** 1125–1136.

Zweifel R, Häsler R. 2001. Dynamics of water storage in mature, subalpine *Picea abies*: temporal and spatial patterns of change in stem radius. *Tree Physiology* **21,** 561–569.

Zweifel R, Item H, Häsler R. 2001. Link between diurnal stem radius changes and tree water relations. *Tree Physiology* **21,** 869–877.

Zweifel R, Zeugin F, Zimmermann L, Newbery DM. 2006. Intra-annual radial growth and water relations of trees: implications towards a growth mechanism. *Journal of Experimental Botany* **57,** 1445–1459.

Zweifel R, Zimmermann L, Newbery DM. 2005. Modeling tree water deficit from microclimate: an approach to quantifying drought stress. *Tree Physiology* **25,** 147–156.